

**The 'Roxolany Tephra' (Ukraine) – new evidence for an origin from Ciomadul volcano, East Carpathians**

Journal:	<i>Journal of Quaternary Science</i>
Manuscript ID	Draft
Wiley - Manuscript type:	Research Article
Date Submitted by the Author:	n/a
Complete List of Authors:	<p>Wulf, Sabine; Senckenberg Research Institute and Natural History Museum, BiK-F, TSP6 Evolution and Climate; Institute for Geosciences, University of Heidelberg</p> <p>Fedorowicz, Stanisław; University of Gdańsk, Institute of Geography, Department of Quaternary Geomorphology and Geology</p> <p>Veres, Daniel; Romanian Academy Institute of Speleology "Emil Racovita"</p> <p>Karátson, David; Eötvös University, Department of Physical Geography</p> <p>Gertisser, Ralf; Keele University, School of Physical and Geographical Sciences</p> <p>Bormann, Marc; University of Cologne, Seminar of Geography and Education</p> <p>Magyari, Enikő; Eötvös University, Department of Physical Geography</p> <p>Appelt, Oona; Helmholtz Centre Potsdam, GFZ German Research Centre for Geosciences, Section 3.3 Chemistry and Physics of Earth Materials</p> <p>Hambach, Ulrich; University of Bayreuth, Lehrstuhl Geomorphologie</p> <p>Łanczont, Maria; Maria Curie-Skłodowska University, Department of Geoecology and Palaeogeography</p> <p>Gozhyk, Petro; National Academy of Sciences of Ukraine, Institute of Geological Sciences</p>
Keywords:	tephra, Roxolany loess, Ukraine, Ciomadul, Lake St. Ana

1  
2  
3 1 **The ‘Roxolany Tephra’ (Ukraine) – new evidence for an origin from Ciomadul volcano,**  
4  
5 2 **East Carpathians**

6  
7 3 Sabine Wulf<sup>1,2\*</sup>, Stanisław Fedorowicz<sup>3</sup>, Daniel Veres<sup>4</sup>, David Karátson<sup>5</sup>, Ralf Gertisser<sup>6</sup>,  
8 4 Marc Bormann<sup>7</sup>, Enikő Magyari<sup>5</sup>, Oona Appelt<sup>8</sup>, Ulrich Hambach<sup>9</sup>, Maria Łanczont<sup>10</sup>, Petro  
9 5 F. Gozhyk<sup>11</sup>

10  
11 6 <sup>1</sup> Senckenberg Research Institute and Natural History Museum, BIK-F, TSP6 Evolution and Climate,  
12 7 Senckenberganlage 25, D-60325 Frankfurt a.M., Germany

13 8 <sup>2</sup> Institute for Geosciences, University of Heidelberg, Im Neuenheimer Feld 234, D-69120 Heidelberg,  
14 9 Germany

15 10 <sup>3</sup> University of Gdańsk, Institute of Geography, Department of Quaternary Geomorphology and  
16 11 Geology, ul. Bażyńskiego 4, 80-950 Gdańsk, Poland

17 12 <sup>4</sup> Romanian Academy Institute of Speleology "Emil Racovita", Clinicilor 5, 400006 Cluj-Napoca,  
18 13 Romania

19 14 <sup>5</sup> Eötvös University, Department of Physical Geography, H-1117 Budapest, Pázmány s. 1/C, Hungary

20 15 <sup>6</sup> School of Physical and Geographical Sciences, Keele University, Keele, Staffordshire, ST5 5BG, United  
21 16 Kingdom

22 17 <sup>7</sup> University of Cologne, Seminar of Geography and Education, Gronewaldstr. 2, D-50931 Cologne, Germany

23 18 <sup>8</sup> Helmholtz Centre Potsdam, GFZ German Research Centre for Geosciences, Section 3.3 Chemistry  
24 19 and Physics of Earth Materials, Telegrafenberg, D-14473 Potsdam, Germany

25 20 <sup>9</sup> BayCEER & Chair of Geomorphology, University of Bayreuth, D-95440 Bayreuth, Germany

26 21 <sup>10</sup> Department of Geoecology and Palaeogeography, Maria Curie-Skłodowska University, Al. Kraśnicka  
27 22 2 cd, 20-718 Lublin, Poland

28 23 <sup>11</sup> Institute of Geological Sciences, National Academy of Sciences of Ukraine, Gonchara 55B, 01 601 Kyiv,  
29 24 Ukraine

30  
31 26 \* **Corresponding author:** [Sabine.Wulf@senckenberg.de](mailto:Sabine.Wulf@senckenberg.de) (S.Wulf), facsimile +49-(0)6221-  
32 27 545503

33  
34  
35 28 **Keywords:** Tephra; Roxolany loess; Ukraine; Ciomadul; Lake St. Ana.

36  
37  
38 29 **Abstract**

39  
40 30 We present major element glass data and correlations of the so-called ‘Roxolany Tephra’ – a  
41 31 so far geochemically unconstrained volcanic ash layer previously described in last glacial  
42 32 (MIS2) loess deposits in SW Ukraine. This exceptional well preserved, 2-3 cm thick tephra  
43 33 shows a rhyolitic glass composition that is comparable with that of proximal tephra units from  
44 34 the Ciomadul volcano in the East Carpathians, central Romania. The chemistry particularly  
45 35 matches that of the final pyroclastic fall unit of Sf. Ana crater that is radiocarbon dated at ca.  
46 36 29.6 cal ka BP. The age of the tephra correlative is in agreement with the newest radiocarbon  
47 37 and OSL age constraints that place it between ca. 33 and 24 cal ka BP within the Roxolany  
48 38 loess sequence and thus confirms the long-debated chronostratigraphic position of the tephra  
49 39 in this important environmental archive. The occurrence of a distal Ciomadul tephra ca. 350

1  
2  
3 40 km east of its source indicates a great potential of further tephra and cryptotephra findings  
4 41 from this volcanic complex in the south-eastern Mediterranean and Black Sea region.  
5  
6

## 7 **1. Introduction**

8  
9  
10 43 The loess-paleosoil complex near the village of Roxolany in the SW Ukraine (Fig. 1) provides  
11 44 an almost complete Pleistocene terrestrial sedimentary record and is thus the most  
12 45 representative sequence for the reconstruction of long-term palaeoclimatic and environmental  
13 46 changes in the Northern Black Sea region. The ca. 48 m thick Roxolany loess sequence was  
14 47 first studied by P. Gozhik with his research team (Putievoditel, 1976; Gozhik *et al.*, 1995),  
15 48 demonstrating its potential for palaeoenvironmental reconstruction on the basis of  
16 49 granulometric, mineralogical, palaeomagnetic, palaeontological (molluscs, mammal fauna)  
17 50 analyses as well as radiocarbon and TL dating. Within these first studies, the authors  
18 51 suggested the Brunhes/Matuyama magnetic reversal (ca. 780 ka) in the lower part of the  
19 52 profile. Later, Tsatskin *et al.* (1998) provided a more detailed description, proposing a revised  
20 53 stratigraphic interpretation of the loess-paleosoil horizons and palaeomagnetic data, and their  
21 54 correlation with the marine oxygen isotope stages (MIS). The authors re-identified the  
22 55 Brunhes/Matuyama boundary in the middle part of the profile in loess unit L<sub>6</sub> at ca. 35 m  
23 56 depth of the Roxolany loess-paleosoil complex, which now enabled a solid correlation with  
24 57 other loess profiles in Europe and China (e.g. Dodonov *et al.*, 2006; Faustov *et al.*, 2009;  
25 58 Gendler *et al.*, 2006; Tsatskin *et al.*, 2001).

26  
27  
28  
29  
30  
31  
32  
33  
34  
35  
36  
37 59 Tsatskin *et al.* (1998) were the first to describe a macroscopic visible tephra (volcanic ash  
38 60 fall) layer, the so-called 'Roxolany Tephra', within the initially proposed L<sub>3</sub> loess unit  
39 61 (corresponding to MIS 12, i.e. the period from 450 to 400 ka; Sartori, 2000). Tephra, in  
40 62 general, are useful chronological and/or synchronisation markers in terrestrial and marine  
41 63 palaeoenvironmental archives, if correlated via glass geochemical fingerprinting with known  
42 64 and dated volcanic events (e.g. Lowe, 2011). Remarkably, Loess-Paleosoil complexes in the  
43 65 Middle and Lower Danube Basin revealed evidence for stratigraphic consistent tephra of  
44 66 diverse stratigraphic position, their precise geochemistry and age, however, is often poorly  
45 67 constraint (e.g. Fitzsimmons *et al.*, 2013; Horváth, 2001; Marković *et al.*, 2015; Panaiotu *et*  
46 68 *al.*, 2001; Veres *et al.*, 2013). Fedorowicz *et al.* (2012) provided a first detailed description of  
47 69 the mineralogical components of the Roxolany Tephra and suggested a possible genetic link  
48 70 with Carpathian volcanic activity. However, this assumption still lacked the geochemical and  
49 71 chronological evidence from proximal and other distal tephra deposits.  
50  
51  
52  
53  
54  
55  
56  
57  
58  
59  
60

1  
2  
3 72 Many years of comprehensive research focusing on Roxolany have brought up a number of  
4  
5 73 new, partially contradicting data in the chronostratigraphic diagnosis of the upper three loess  
6  
7 74 units (Fig. 2), and implicitly the timing of tephra deposition varied depending on such  
8  
9 75 interpretations (Boguckiyi *et al.* (eds), 2013; Gozhik *et al.*, 2007; Putivnyk, 2000). According  
10  
11 76 to the newest data, the ‘Roxolany Tephra’ is embedded within the Bug loess (bg) from the  
12  
13 77 upper pleniglacial of the Weichselian glaciation (MIS 2) (Gozhik *et al.*, 2007) (Fig. 2). It is  
14  
15 78 overlain by two paleosol layers of an interphase rank, the *Prychornomorsk* (pc) and the  
16  
17 79 *Dofinivka* (df) units, that have recently been radiocarbon dated at ca. 23.5 cal ka BP and 34.7  
18  
19 80 cal ka BP, respectively (Boguckiyi *et al.* (eds), 2013; Fedorowicz *et al.*, 2012) (Fig. 2). The  
20  
21 81 paleosol underlying the tephra-bearing bg loess, the *Vytachiv* (vt) unit, has been attributed to  
22  
23 82 the middle Pleniglacial (MIS 3) and is AMS radiocarbon dated between 21 and 25.5 cal ka BP  
24  
25 83 (Boguckiyi *et al.* (eds), 2013; Fedorowicz *et al.*, 2012) (Fig. 2). Optically-stimulated  
26  
27 84 luminescence (OSL) dates of loess samples from ca. 9 m below the tephra revealed an age of  
28  
29 85  $33.1 \pm 2.6$  ka (Boguckiyi *et al.* (eds), 2013; Fedorowicz *et al.*, 2012), confirming both the  
30  
31 86 radiocarbon-based chronology and the stratigraphic scheme developed by Gozhik *et al.* (1995;  
32  
33 87 2007) pointing to very high accumulation rates, that also favoured tephra preservation within  
34  
35 88 loess. Further attempts to directly date phenocrysts of the Roxolany Tephra, however, led to  
36  
37 89 unrealistic old ages of  $50 \pm 3$  Ma ( $^{40}\text{Ar}/^{39}\text{Ar}$ ; Sartori, 2000; Tsatskin *et al.*, 1998) and 11.83-  
38  
39 90 14.54 Ma (K/Ar on amphibole and biotite; Fedorowicz *et al.*, 2012).

35  
36 91 In this study, we provide the first geochemical glass data of the ‘Roxolany Tephra’ and a solid  
37  
38 92 correlation scheme with its dated volcanic source as a contribution to (1) the clarification of  
39  
40 93 the chronostratigraphy of the Roxolany loess-paleosol complex, and (2) the extension of the  
41  
42 94 tephrostratigraphical framework in south-eastern Europe with the principal aim at providing  
43  
44 95 means for comparing various records on a wider scale.  
45  
46 96

## 97 **2. Samples and methods**

### 98 *2.1 Roxolany sampling site*

99 The Roxolany outcrop is situated on the eastern bank of the Dniester estuary, about 40 km  
100 southwest of Odessa and ca. 1.5 km northwest of the village of Roxolany, SW Ukraine  
101 ( $46^{\circ}10'N$ ,  $30^{\circ}27'E$ ) (Fig. 1). The ca. 48 m thick Loess-Paleosol complex crops out along the  
102 ‘Zayach’ya Balka’ gully, which is deeply incised into the sedimentary mantle of the VII  
103 Dniester terrace containing the late Tamaian mammal complex (Chepalyga, 1967; Putivnyk,

1  
2  
3 104 2000; Gozhik *et al.*, 2007). A sample was taken from the 2-3 cm thick, white-greyish tephra  
4 105 layer that occurs in the third upper loess unit at ca. 9.5 m depth (Fig. 2).  
5  
6 106

## 7 107 *2.2 Tephrochronological methods*

8 108 The tephra sample from the Roxolany loess sequence was treated with a 15% hydrogen  
9 109 peroxide (H<sub>2</sub>O<sub>2</sub>) solution to remove organic remains and subsequently wet-sieved into a 32-  
10 110 125 µm grain size fraction. Dried tephra components were embedded on a slide with  
11 111 Araldit©2020 resin, sectioned by hand on silicon paper, polished and finally carbon coated  
12 112 for electron probe microanalyses (EPMA). The major element composition of single glass  
13 113 shards was determined at a CAMECA SX-100 and a JEOL-JXA8230 instrument at the GFZ  
14 114 Potsdam using a 15 kV voltage, a 20 nA and 10 nA beam current and a beam size of 15 µm  
15 115 and 8 µm, respectively. Exposure times were 20 seconds for the elements Fe, Cl, Mn, Ti, Mg  
16 116 and P, as well as 10 seconds for F, Si, Al, K, Ca and Na. Instrumental calibration used natural  
17 117 minerals and the rhyolitic Lipari obsidian glass standard (Hunt and Hill, 1996; Kuehn *et al.*,  
18 118 2011). Glass data are reported in Table 1 and compared in bivariate plots with published  
19 119 EPMA glass data of potential tephra correlatives (Figs. 3, 4).  
20

21 120 Back-scattered electron (BSE) images of volcanic glass shards from different grain size  
22 121 fractions (32-63 µm, 63-125 µm and >125 µm) were acquired with a 15 kV accelerating  
23 122 voltage with a Hitachi TM3000 Tabletop Scanning Electron Microscope (SEM) at Keele  
24 123 University.  
25

## 26 124

### 27 125 **3. Composition of the Roxolany tephra**

28 126 The Roxolany Tephra is a fine-grained ( $d_{\max} = 200 \mu\text{m}$ ) volcanic ash that is dominated by  
29 127 lithics, plagioclase, green pyroxene and biotite crystals (Fig. 3A). It also consists of highly  
30 128 vesicular, microcryst-rich (feldspars, pyroxenes) pumices (Fig. 3B) and blocky, low-vesicular  
31 129 glass shards (Figs. 3C, 3D) that indicate an phreatomagmatic origin. Due to the mean low  
32 130 analytical totals of ca. 94-95 wt%, volcanic glasses are interpreted to be slightly altered (Table  
33 131 1). Analytical data from both EPMA instruments using different setups are comparable with  
34 132 each other except for slightly higher SiO<sub>2</sub> and lower Al<sub>2</sub>O<sub>3</sub> values for the JEOL probe data  
35 133 that used a smaller beam size (Table 1). Accordingly, the major element glass composition is  
36 134 calc-alkaline rhyolitic with SiO<sub>2</sub> and Al<sub>2</sub>O<sub>3</sub> concentrations of 75.6-77.6 wt% and 12.9-14.0  
37 135 wt% (normalized, volatile-free data), respectively. Concentrations in FeO (0.5-0.9 wt%) and  
38 136 CaO (0.8-1.1 wt%) are low, and alkali ratios (K<sub>2</sub>O/Na<sub>2</sub>O) vary between 1.1 and 1.5 (Figs. 4  
39 137 and 5).  
40  
41  
42  
43  
44  
45  
46  
47  
48  
49  
50  
51  
52  
53  
54  
55  
56  
57  
58  
59  
60

138

#### 4. Source and associated age of the Roxolany Tephra

The glass composition of the Roxolany Tephra was compared to EPMA glass data of other Late Pleistocene tephtras occurring in the Eastern Mediterranean. Calc-alkaline rhyolitic tephtras were produced from several volcanic centres of the Aeolian (Italy) and Aegean Arcs (Greece), Anatolia (Turkey) and the East Carpathians (Romania) during the considered time span between ca. 50 and 20 ka (Fig. 1).

Lipari Island in southern Italy (ca. 1530 km SW of Roxolany), for example, erupted the Monte Guardia rhyolites between 27 and 24 cal ka BP (e.g. Forni *et al.*, 2013). However, this sub-plinian eruption had only limited regional tephtra dispersal (e.g. Crisci *et al.*, 1991; Forni *et al.*, 2013; Lucchi *et al.*, 2008), and the respective juvenile pyroclasts show a distinct major-element composition with lower concentrations in SiO<sub>2</sub> and higher FeO concentrations compared to the Roxolany Tephtra (Fig. 4).

The Lower and Upper Pumices from Nisyros (Aegean Arc, ca. 1100 km SSW of Roxolany) are dated at >50 ka (Margari *et al.*, 2007; Tomlinson *et al.*, 2012; Karkanis *et al.*, 2015) and show a similar glass composition to the Roxolany Tephtra except for higher FeO and slightly lower Al<sub>2</sub>O<sub>3</sub> values. Both Nisyros tephtras have been found as discrete layers in marine sites south of the vent (Keller *et al.*, 1978), but were not identified in northern locations so far except for the Upper Pumice recently reported as a cryptotephtra within the Theopetra cave, stratigraphically overlain by the Pantellerian Y6/Green Tuff, dated to 45.7 ka (Karkanis *et al.*, 2015). In the more proximal marine stratigraphy, the Upper Nisyros Pumices are overlain by the ca. 31 ka Yali-C (Yali-2) tephtra (Federman and Carey, 1980), which in turn has a limited regional dispersal and a distinct rhyolitic composition compared to the Roxolany tephtra (Fig. 4). The Y-2/Cape Riva tephtra (22 cal ka BP) from Thera volcano (Santorini, Aegean Arc, ca. 1150 SSW of Roxolany) has been widely distributed towards the north (>500 km) and the northeast (>700 km) (e.g. Kwiecien *et al.*, 2008; Müller *et al.*, 2011; Wulf *et al.*, 2002). However, the glass chemical composition of the Y-2 tephtra is less silicic rhyolitic (Fig. 4), and thus this tephtra can be excluded as a potential correlative of the Roxolany Tephtra.

Anatolian stratovolcanoes and caldera complexes, i.e. Acigöl and Erciyes Dağ (Central Anatolian Volcanic Province CAVP, ca. 900-950 km SSE of Roxolany), and Süphan and Nemrut Dagi (East Anatolian Volcanic Province EAVP, ca. 1280 km SE of Roxolany), produced numerous pyroclastic fallout deposits of highly silicic rhyolitic glass compositions during the considered time frame (e.g. Deniel *et al.*, 1998; Druitt *et al.*, 1995; Kuzucuoglu *et al.*, 1998; Sumita and Schmincke, 2013b) (Fig. 4). Especially the MIS2 tephtras from Acigöl

1  
2  
3 172 and Süphan Dagi come close to the major-element composition of the Roxolany Tephra (Fig.  
4 173 4). Those tephtras, however, have so far only been recognized close to their volcanic centres  
5 174 (e.g. visible tephra layers from Süphan in Lake Van sediments; Schmincke *et al.*, 2014;  
6 175 Sumita and Schmincke, 2013a) and potentially as cryptotephra layers (macroscopic non-  
7 176 visible tephra layers) in south-eastern Black Sea sediments (Cullen *et al.*, 2014) (Figs. 1 and  
8 177 5). Other CAVP tephtras that show compositions comparable to the Roxolany Tephra, e.g.  
9 178 early Holocene deposits from Erciyes Dağ, are dispersed towards the south (Develle *et al.*,  
10 179 2009; Hamann *et al.*, 2010) and too young to be considered as correlatives.

11 180 The large thickness and maximum grain sizes of the Roxolany tephra, however, suggest a  
12 181 rather nearby source, e.g. the southern East Carpathians. New chronostratigraphic data of the  
13 182 latest pyroclastic deposits of the Ciomadul andesitic-dacitic lava dome complex in the East  
14 183 Carpathians (Romania, ca. 350 km W of Roxolany; Fig. 1) indicate that this site was indeed  
15 184 explosively active (e.g. Harangi *et al.*, 2015; Karátson *et al.*, 2013; Szakács and Seghedi,  
16 185 1990, 1995), especially during its final eruptive stage at 52-29 ka BP (Karátson *et al.*,  
17 186 submitted). The last eruptions of Ciomadul were characterized by successive crater  
18 187 formations (e.g. Mohoš, St. Ana) and by widespread dispersal of at least three tephra units  
19 188 (Karátson *et al.*, submitted). The phreatomagmatic 'Turia' (ca. 52 ka) and plinian 'TGS'  
20 189 deposits (ca. 31.5 ka), for example, are widely dispersed towards the southeast (Karátson *et*  
21 190 *al.*, submitted). The final phreatomagmatic LSA eruption likely originated from the St. Ana  
22 191 crater and is radiocarbon dated on the basis of lacustrine deposits of the Mohoš and St. Ana  
23 192 craters at  $\geq 29.6 \pm 0.6$  cal ka BP and  $> 27$  cal ka BP, respectively (Karátson *et al.*, submitted).  
24 193 The dispersal direction of the LSA tephra has been tentatively proposed towards the east  
25 194 (Karátson *et al.*, submitted; Veres *et al.*, in prep.). Glass chemical data show a distinct and  
26 195 relatively heterogeneous rhyolitic composition for all three Ciomadul tephtras, with the oldest  
27 196 Turia tephra being the most evolved (mean high SiO<sub>2</sub> values of ca. 78 wt%) and the TGS  
28 197 tephra the least silicic products (mean SiO<sub>2</sub> concentration of ca. 73 wt%) (Fig. 5). Major-  
29 198 element glass data of the chemically intermediate LSA tephra (mean SiO<sub>2</sub> values of 76.5  
30 199 wt%), especially those of the uppermost dated tephra layer RO-1/2/3 in the Mohoš core  
31 200 (Karátson *et al.*, submitted), show the best agreement with the glass data of the Roxolany  
32 201 Tephra (Fig. 5). The chemical correlation with the LSA tephra is furthermore supported by  
33 202 the thickness and maximum grain sizes of the Roxolany Tephra, which imply a transport from  
34 203 the St. Ana crater over a relatively short distance ( $> 350$  km) and by favourable westerly  
35 204 winds, the prevailing atmospheric circulation in the region. The correlation of the Roxolany  
36 205 Tephra with the final eruptive products of Ciomadul volcano, in turn, confirms the proposed

206 time constraints (33-24 cal ka BP) of tephra embedding loess deposits at Roxolany during the  
207 last Glacial Maximum (Fig. 2).

208

## 209 **5. Implication for the distal tephrostratigraphy of Ciomadul volcano**

210 The identification of the LSA tephra from Ciomadul volcano at the distal site of Roxolany has  
211 further implications on the tephrostratigraphic framework of the Eastern Mediterranean –  
212 Black Sea region, particularly for the linking of the widespread loess records, whose detailed  
213 correlation is still hampered by limited chronological control (Veres *et al.*, 2013; Markovic *et*  
214 *al.*, 2015). The finding of a 2-3 cm thick tephra layer indicates on the one hand an exceptional  
215 preservation in loess sediments, probably due to high sedimentation rates and related rapid  
216 covering of the tephra by wind-blown sediments (Chlebowski *et al.*, 2003; Boguckyi *et al.*  
217 (eds), 2013). This minimum thickness in combination with the relatively large grain sizes of  
218 tephra components at ca. 350 km distance suggests an origin from a violent, even  
219 phreatoplinian eruption and a widespread dispersal of the LSA tephra by strong westerly  
220 winds. We thus expect further LSA tephra and cryptotephra findings beyond the Roxolany  
221 site (e.g. in Eastern Romania, Ukraine and southern Russia) in the near future. Similarly, a  
222 wider dispersal of the older Turia and TGS tephtras from Ciomadul in a southerly/south-  
223 easterly direction, i.e. at sites in southern Romania, the Balkans, the Black Sea and beyond,  
224 can be anticipated. Sediment core M72/5-25-GC1 from the south-eastern Black Sea (Fig.1),  
225 located ca. 1050 km ESE of Ciomadul, has already been proposed as such a potential site of  
226 Ciomadul cryptotephra preservation, but no solid tephra correlation was possible so far  
227 (Cullen *et al.*, 2014). The comparison of new major-element glass chemical and  
228 chronostratigraphic data from Ciomadul's latest stage activity with 48.3-25 ka cryptotephra  
229 data of the Black Sea core (BSC) also only allows tentative correlations (Fig. 4). For instance,  
230 the less evolved glass population of cryptotephra BSC\_651, dated between 25 ka and  
231 34.4±0.65 ka (Cullen *et al.*, 2014; Nowaczyk *et al.*, 2012), has a strong affinity to the 31.5 ka  
232 TGS tephra except for the lower CaO concentrations (Fig. 4). Older cryptotephtras from the  
233 Black Sea core dated between 34.4 ka and 48.3 ka are geochemically indistinctive from each  
234 other, the Turia tephtras from Ciomadul and EAPV (Süphan) tephtras (Figs. 3,4). In these  
235 cases, trace element and isotopic data sets of glass shards from all – proximal and distal –  
236 archives will be required for further detangling.

237

## 238 **6. Summary and Conclusions**

1  
2  
3 239 The tephrochronological study of the Roxolany loess site in combination with new  
4  
5 240 geochemical and chronostratigraphic tephra constraints from the latest stage activity of  
6  
7 241 Ciomadul volcano (East Carpathians) allow a robust correlation of the long-discussed  
8  
9 242 Roxolany Tephra with the final LSA eruption of Ciomadul. The age of the LSA tephra is  
10  
11 243 constrained at the source volcano at ca. 29.6 cal ka BP and is in good agreement with the  
12  
13 244 latest dates obtained for the Roxolany Tephra embedding sediments. Therefore, the Roxolany  
14  
15 245 Tephra was deposited during the onset of the glacial maximum of the Weichselian phase, a  
16  
17 246 period of intense aeolian activity. The occurrence of a visible Ciomadul tephra layer ca. 350  
18  
19 247 km east of its vent has important implications for future (crypto) tephra findings in the south-  
20  
21 248 eastern Mediterranean and Black Sea region that would integrate the Carpathian volcanism  
22  
23 249 into the building of a regional tephra framework focusing on linking terrestrial (loess and  
24  
25 250 alluvial) and marine records.  
26  
27 251

## 252 **Acknowledgements**

253 This study was supported by the projects No. NN306 474138 and No. 691-N/2010/0  
254  
255 Ukraine of the Polish Ministry of Science and Higher Education. Furthermore, financial  
256  
257 support by Hungarian National Funds K115472 and NF101362 was provided. D.V.  
258  
259 acknowledges the support by a grant of the Ministry of National Education, CNCS–  
260  
261 UEFISCDI, project number PN-II-ID-PCE-2012-4-0530.

## 262 **References**

- 263 Boguckyi A, Gozhik P, Lanczont M, Madeyska T, Jelovichowa J (eds). 2013. Loess cover in  
264  
265 the north Black Sea area. *XVIII Polish-Ukrainian Seminar*. KARTPOL s.c. Lublin, Roxolany,  
266  
267 268 pp.
- 268 Çağatay MN, Wulf S, Ümmühan S, Özmaral A, Vidal L, Henry P, Appelt O, Gasperini L.  
269  
270 2015. The tephra record from the Sea of Marmara for the last ca. 70 ka and its  
271  
272 palaeoceanographic implications. *Marine Geology* **361** : 96-110.
- 273 Chepalyga AL. 1967. Antropogenovye presnovodnye molyuski Yuga Russkoi ravniny i ikh  
274  
275 stratigraficheskoye znachenie [ Quaternary fresh-water molluscs in the South of the Russian  
276  
277 plain and their stratigraphic importance]. *Nauka*, Moscow, 222 pp.
- 278 Chlebowski R, Gozhik P, Lindner L, Lanczont M, Wojtanowicz J. 2003. Stratigraphy and  
279  
280 sedimentology of the Bug loess (Pleistocene: Upper Vistulian) between Kiev and Odessa  
281  
282 (Ukraine). *Geological Quarterly* **47** : 261-268.

- 1  
2  
3 274 Crisci GM, De Rosa R, Esperanca S, Mazzuoli R, Sonnino M. 1991. Temporal evolution of a  
4 275 three component system: the island of Lipari (Aeolian Arc, southern Italy). *Bulletin of*  
5 276 *Volcanology* **53** : 207-221.
- 7 277 Cullen VL, Smith VC, Arz HW. 2014. The detailed tephrostratigraphy of a core from the  
8 278 south-east Black sea spanning the last ~ 60 ka. *Journal of Quaternary Science* **29** : 675-690.
- 10 279 Deniel C, Aydar E, Gourgau A. 1998. The Hasan Dagi stratovolcano (Central Anatolia,  
11 280 Turkey): evolution from calc-alkaline to alkaline magmatism in a collision zone. *Journal of*  
12 281 *volcanology and Geothermal Research* **87** : 275-302.
- 14 282 Develle A-L, Williamson D, Gasse F, Walter-Simonnet A-V. 2009. Early Holocene volcanic  
15 283 ash fallout in the Yammoûneh lacustrine basin (Lebanon): Tephrochronological implications  
16 284 for the Near East. *Journal of Volcanology and Geothermal Research* **186** : 416-425.
- 18 285 Dodonov AE, Zhou LP, Markova AK, Tchepalyga AL, Trubikhin VM, Aleksandrovski AL,  
19 286 Simakova AN. 2006. Middle – Upper Pleistocene bio-climatic and magnetic records of the  
20 287 Northern Black Sea Coastal Area. *Quaternary International* **149** : 44–54.
- 22 288 Druitt TH, Brenchley PJ, Gökten YE, Francaviglia V. 1995. Late Quaternary rhyolitic  
23 289 eruptions from the Acigöl Complex, central Turkey. *J. Geol. Soc., London* **152** : 655-667.
- 25 290 Faustov SS, Virina EI, Tsatskin A, Gendler TS, Heller F. 2009. The Matuyama/Brunhes  
26 291 boundary in loess sections in the south of the East European Plain and their correlation on the  
27 292 basis of palaeomagnetic and palaeopedologic data. *Quaternary International* **201** : 60-66.
- 29 293 Federman AN, Carey SN. 1980. Electron microprobe correlation of tephra layers from  
30 294 Eastern Mediterranean abyssal sediments and the island of Santorini. *Quaternary Research* **13**  
31 295 : 160 - 171.
- 33 296 Fedorowicz S, Wozniak PP, Halas S, Lanczont M, Paszkowski M, Wójtowicz A. 2012.  
34 297 Challenging K-Ar dating of the Quaternary tephra from Roxolany, Ukraine. *Mineralogia -*  
35 298 *Special Papers* **39** : 102-105.
- 37 299 Fitzsimmons K, Hambach U, Veres D, Iovita R. 2013. The Campanian Ignimbrite eruption:  
38 300 new data on volcanic ash dispersal and its potential impact on human evolution. *PLoS One*  
39 301 **8/6**: e65839. <http://dx.doi.org/10.1371/journal.pone.0065839>
- 42 302 Forni F, Lucchi F, Peccerillo A, Tranne CA, Rossi PL, Frezzotti ML. 2013. Stratigraphy and  
43 303 geological evolution of the Lipari volcanic complex (central Aeolian archipelago). *Geological*  
44 304 *Society, London, Memoirs* **37** : 213-279.
- 46 305 Gendler TS, Heller F, Tsatskin A, Spassov S, Du Pasquier J, Faustov SS. 2006. Roxolany and  
47 306 Novaya Etuliya - key sections in the western Black Sea loess area: Magnetostratigraphy, rock  
48 307 magnetism, and paleopedology. *Quaternary International* **152-153** : 78-93.
- 50 308 Gozhik P, Shelkopyas V, Khristoforova T. 1995. Development stages of loessial and facial  
51 309 formation in Ukraine (Stratigraphy of loess in Ukraine). Lublin. *Annales Universitatis Mariae*  
52 310 *Curie-Sclodowska. Sec. B.* **50** : 65–74.
- 54 311 Gozhik P, Komar M, Krohmal O, Shelkopyas V, Khristoforova T, Dykan N, Prylypko S.  
55 312 2007. The key section of Neopleistocene subaerial deposits near Roxolany village (Odessa  
56 313 region). *Problemy serednoplejstocenogo interglacialu.* Lviv, Vid. Centr. LNU im. I. Franka,  
57 314 pp. 109-128.

- 1  
2  
3 315 Hamann Y, Wulf S, Ersoy O, Ehrmann W, Aydar E, Schmiedl G. 2010. First evidence of a  
4 316 distal early Holocene ash layer in Eastern Mediterranean deep-sea sediments derived from the  
5 317 Anatolian volcanic province. *Quaternary Research* **73** : 497-506.
- 6  
7 318 Harangi S, Lukács R, Schmitt AK, Dunkl I, Molnár K, Kiss B, Seghedi I, Novothny Á,  
8 319 Molnár M. 2015. Constraints on the timing of Quaternary volcanism and duration of magma  
9 320 residence at Ciomadul volcano, east-central Europe, from combined U-Th/He and U-Th  
10 321 zircon geochronology. *Journal of Volcanology and Geothermal Research* **301** : 66-80.
- 11  
12 322 Horváth E. 2001. Marker horizons in the loesses of the Carpathian Basin. *Quaternary*  
13 323 *International* **76** : 157-163.
- 14  
15 324 Hunt JB, Hill PG. 1996. An inter-laboratory comparison of the electron probe microanalysis  
16 325 of glass geochemistry. *Quaternary International* **34-36** : 229-241.
- 17  
18 326 Karátson D, Telbisz T, Harangi S, Magyar E, Dunkl I, Kiss B, Jánosi C, Veres D, Braun M,  
19 327 Fodor E, Biró T, Kósik S, von Eynatten H, Lin D. 2013. Morphometrical and  
20 328 geochronological constraints on the youngest eruptive activity in East-Central Europe at the  
21 329 Ciomadul (Csomád) lava dome complex, East Carpathians. *Journal of Volcanology and*  
22 330 *Geothermal Research* **255** : 43-56.
- 23  
24 331 Karátson D, Wulf S, Veres D, Magyar EK, Gertisser R, Timar-Gabor A, Novothny Á,  
25 332 Telbisz T, Szalai Z, Anechitei-Deacu V, Appelt O, Bormann M, Jánosi C, Hubay K, Schäbitz  
26 333 F. submitted. The latest explosive eruptions of Ciomadul (Csomád) volcano, East Carpathians  
27 334 - a tephrostratigraphic approach for the 52-29 ka BP time interval. *Journal of Volcanology*  
28 335 *and Geothermal Research*.
- 29  
30 336 Karkanias P, White D, Lane CS, Stringer C, Davies W, Cullen VL, Smith VC, Ntinou M,  
31 337 Tsartsidou G, Kyriasi-Apostolika N. 2015. Tephra correlations and climatic events between  
32 338 the MIS6/5 transition and the beginning of MIS3 in Theopetra Cave, central Greece.  
33 339 *Quaternary Science Reviews* **188** : 170-181.
- 34  
35 340 Keller J, Ryan WBF, Ninkovich D, Altherr R. 1978. Explosive volcanic activity in the  
36 341 Mediterranean over the past 200,000 yr as recorded in deep-sea sediments. *Geological Society*  
37 342 *of America Bulletin* **89** : 591 - 604.
- 38  
39 343 Kuehn SC, Froese DG, Shane PAR, INTAV Intercomparison Participants. 2011. The INTAV  
40 344 intercomparison of electron-beam microanalysis of glass by tephrochronology laboratories:  
41 345 Results and recommendations. *Quaternary International* **246** : 19-47.
- 42  
43 346 Kuzucuoglu C, Pastre J-F, Black S, Ercan T, Fontugne M, Guillou H, Hatté C, Karabiyikoglu  
44 347 M, Orth P, Türkecan A. 1998. Identification and dating of tephra layers from Quaternary  
45 348 sedimentary sequences of Inner Anatolia, Turkey. *Journal of Volcanology and Geothermal*  
46 349 *Research* **85** : 153-172.
- 47  
48 350 Kwiecien O, Arz HW, Lamy F, Wulf S, Bahr A, Röhl U, Haug GH. 2008. Estimated reservoir  
49 351 ages of the Black Sea since the Last Glacial. *Radiocarbon* **50** : 1-20.
- 50  
51 352 Lowe DJ. 2011. Tephrochronology and its application: A review. *Quaternary Geochronology*  
52 353 **6** : 107-153.
- 53  
54 354 Lucchi F, Tranne CA, De Astis G, Keller J, Losito R, Morche W. 2008. Stratigraphy and  
55 355 significance of Brown Tuffs on the Aeolian Islands (southern Italy). *Journal of Volcanology*  
56 356 *and Geothermal Research* **177** : 49-70.

- 1  
2  
3 357 Margari V, Pyle DM, Bryant C, Gibbard PL. 2007. Mediterranean tephra stratigraphy  
4 358 revisited: Results from a long terrestrial sequence on Lesvos Island, Greece. *Journal of*  
5 359 *Volcanology and Geothermal Research* **163** : 34-54.  
6  
7 360 Marković SB, Stevens T, Kukla GJ, Hambach U, Fitzsimmons KE, Gibbard P, Buggle B,  
8 361 Zech M, Guo Z, Hao Q, Wu H, O'Hara Dhand K, Smalley IJ, Újvári G, Sümegi P, Timar-  
9 362 Gabor A, Veres D, Sirocko F, Vasiljević DA, Jary Z, Svensson A, Jović V, Lehmkühl F,  
10 363 Kovács J, Svirčev Z. 2015. Danube loess stratigraphy — Towards a pan-European loess  
11 364 stratigraphic model. *Earth-Science Reviews* **148** : 228-258.  
12  
13 365 Müller UC, Pross J, Tzedakis PC, Gamble C, Kotthoff U, Schmiedl G, Wulf S, Christanis K.  
14 366 2011. The role of climate in the spread of modern humans into Europe. *Quaternary Science*  
15 367 *Reviews* **30** : 273-279.  
16  
17 368 Nowaczyk NR, Arz HW, Frank U, Kind J, Plessen B. 2012. Dynamics of the Laschamp  
18 369 geomagnetic excursion from Black Sea sediments. *Earth and Planetary Science Letters* **351-**  
19 370 **352** : 54-69.  
20  
21 371 Panaiotu CG, Panaiotu EC, Grama A, Necula C. 2001. Paleoclimatic record from a loess-  
22 372 paleosol profile in southeastern Romania. *Physics and Chemistry of the Earth, Part A: Solid*  
23 373 *Earth and Geodesy* **26(11)** : 893-898.  
24  
25 374 Putievoditel X. 1976. VIII mezhdunarodnogo symozjuma po lessovym porodam Kiev-  
26 375 Odessa. Guidebook, Naukova dumka, 46 pp.  
27  
28 376 Putivnyk X. 2000. X polsko-ukrainskogo seminaru Korelacija lesiv i lodovykovykh vidkladiv  
29 377 Polzi i Ukrainy. Guidebook, *ING NAN Ukrainy*, Kiev, 36 pp.  
30  
31 378 Sartori M. 2000. The Quaternary climate in loess sediments: Evidence from rock and mineral  
32 379 magnetic and geochemical analysis. PhD Thesis, Swiss Federal Institute of Technology,  
33 380 Zurich, Switzerland, 231 pp.  
34  
35 381 Schmincke H-U, Sumita M, Paleovan scientific team. 2014. Impact of volcanism on the  
36 382 evolution of Lake Van (eastern Anatolia) III: Periodic (Nemrut) vs. episodic (Süphan)  
37 383 explosive eruptions and climate forcing reflected in a tephra gap between ca. 14 ka and ca. 30  
38 384 ka. *Journal of Volcanology and Geothermal Research* **285** : 195-213.  
39  
40 385 Sumita M, Schmincke H-U. 2013a. Impact of volcanism on the evolution of Lake Van I:  
41 386 evolution of explosive volcanism of Nemrut Volcano (eastern Anatolia) during the past  
42 387 >400,000 years. *Bulletin of Volcanology* **75** : 714.  
43  
44 388 Sumita M, Schmincke H-U. 2013b. Impact of volcanism on the evolution of Lake Van II:  
45 389 Temporal evolution of explosive volcanism of Nemrut Volcano (eastern Anatolia) during the  
46 390 past ca. 0.4 Ma. *Journal of Volcanology and Geothermal Research* **253** : 15-34.  
47  
48 391 Szakács A, Seghedi I. 1990. Quaternary dacitic volcanism in the Ciomadul massif (South  
49 392 Harghita Mts, East Carpathians, Romania. *IAVCEI International Volcanological Congress*,  
50 393 Mainz, Germany.  
51  
52 394 Szakács A, Seghedi I. 1995. Time-space evolution of Neogene-Quaternary volcanism in the  
53 395 Calimani-Gurghiu-Harghita volcanic chain. Guide to excursion B3, IUGS, Regional  
54 396 committee on Mediterranean Neogene stratigraphy, Romania. *Journal of Stratigraphy* **76** : 24  
55 397 pp.  
56  
57  
58  
59  
60

398 Tomlinson EL, Kinvig HS, Smith VC, Blundy JD, Gottsmann J, Müller W, Menzies MA.  
 399 2012. The Upper and Lower Nisyros Pumices: Revisions to the Mediterranean  
 400 tephrostratigraphic record based on micron-beam glass geochemistry. *Journal of Volcanology*  
 401 *and Geothermal Research* **243-244** : 69-80.

402 Tomlinson EL, Smith VC, Albert PG, Aydar E, Civetta L, Cioni R, Cubukcu E, Gertisser R,  
 403 Isaia R, Menzies MA, Orsi G, Rosi M, Zanchetta G. 2015. The major and trace element glass  
 404 compositions of the productive Mediterranean volcanic sources: tools for correlating distal  
 405 tephra layers in and around Europe. *Quaternary Science Reviews* **118** : 48-66.

406 Tsatskin A, Heller F, Gendler TS, Virina EI, Spassov S, Du Pasquier J, Hus J, Hailwood EA,  
 407 Bagin VI, Faustov SS. 2001. A new scheme of terrestrial paleoclimate evolution during the  
 408 last 1.5 Ma in the western Black Sea region: integration of soil studies and loess magmatism.  
 409 *Physics and Chemistry of the Earth* **26** : 911-916.

410 Tsatskin A, Heller F, Hailwood EA, Gendler TS, Hus J, Montgomery P, Sartori M, Virina EI.  
 411 1998. Pedosedimentary division, rock magnetism and chronology of the loess/palaeosol  
 412 sequence at Roxolany (Ukraine). *Palaeogeography, Palaeoclimatology, Palaeoecology* **143** :  
 413 111-133.

414 Veres D, Lane CS, Timar-Gabor A, Hambach U, Constantin D, Szakacs A, Fülling A, Onac  
 415 BP. 2013. The Campanian Ignimbrite/Y5 tephra layer: A regional stratigraphic marker for  
 416 Isotope Stage 3 deposits in the Lower Danube region, Romania. *Quaternary International* **293**  
 417 : 22-33.

418 Vinci A. 1985. Distribution and chemical composition of tephra layers from Eastern  
 419 Mediterranean abyssal sediments. *Marine Geology* **64** : 143-155.

420 Wulf S, Kraml M, Kuhn T, Schwarz M, Inthorn M, Keller J, Kuscu I, Halbach P. 2002.  
 421 Marine tephra from the Cape Riva eruption (22 ka) of Santorini in the Sea of Marmara.  
 422 *Marine Geology* **183** : 131-141.

423

424

425

#### 426 **Figure captions**

427

428 **Figure 1.** Landsat image (Google Earth 2015) of the central and eastern Mediterranean  
 429 showing the location of main silicic volcanic centres and sites mentioned in the text. Left inlet  
 430 map: Landsat image of the Ciomadul volcanic complex with St. Ana and Mohoş craters.  
 431 Right inlet map: location of the Roxolany sampling site (red arrow).

432

433 **Figure 2:** Stratigraphy, lithology and dating results for the upper loess section at Roxolany.

434 (A) General overview of the top loess-soil section with position of the volcanic ash layer. (B)

1  
2  
3 435 MIS2 sediments at the Roxolany site, showing the Dofinivka soils (red-brownish top layer)  
4  
5 436 and upper section of the Bug loess unit that contains the 2-3 cm thick white-greyish Roxolany  
6  
7 437 tephra.  
8

9  
10 438

11 439 **Figure 3:** Backscatter electron (BSE) images of Roxolany Tephra components. Overview of  
12  
13 440 the 63-125  $\mu\text{m}$  grain size fraction (A); highly vesicular, microcryst-rich pumice of the >125  
14  
15 441  $\mu\text{m}$  fraction (B); low-vesicular, microcryst-rich glass shards (C) with attached feldspar  
16  
17 442 phenocrystal (D) of the 63-125  $\mu\text{m}$  fraction. gl = volcanic glass; fs = feldspar; lt = lithic.  
18  
19

20  
21 443

22  
23 444 **Figure 4:** Geochemical bivariate plots of glass data of the Roxolany tephra in comparison to  
24  
25 445 published data of potential central and eastern Mediterranean tephra sources. EPMA data are  
26  
27 446 obtained from: Roxolany tephra (red stars): this study; Lipari: Crisci *et al.* (1991); Cape  
28  
29 447 Riva/Y-2, Santorini: Çağatay *et al.* (2015), Tomlinson *et al.* (2015), Wulf *et al.* (2002); Yali-  
30  
31 448 C: Federman and Carey (1980), Vinci (1985); Nisyros Lower and Upper Pumices: Tomlinson  
32  
33 449 *et al.* (2012); Erciyes Dag and Acigöl: Tomlinson *et al.* (2015); Süphan Dagi and Nemrut  
34  
35 450 Dagi: Schmincke *et al.* (2014).  
36  
37

38  
39 451

40  
41 452 **Figure 5:** Geochemical bivariate plots of glass data for discriminating between the Roxolany  
42  
43 453 tephra (red stars, this study), proximal tephra deposits (Turia, TGS, LSA including sample  
44  
45 454 RO-1/2/3) from the latest activity of Ciomadul volcano (Karátson *et al.*, submitted) and Black  
46  
47 455 Sea Core (BSC) cryptotephra of the last Glacial (Cullen *et al.*, 2014).  
48  
49

50 456

#### 51 457 **Table captions**

52  
53  
54 458 **Table 1:** EPMA raw data of single point glass analyses, mean values and  $2\sigma$  standard  
55  
56 459 deviation (*sd*) of the Roxolany tephra, and results of the rhyolitic Lipari Obsidian glass  
57  
58 460 standard.  
59  
60

461

462 **Table 1:**

463

**CAMECA SX-100 (23/07/2004)**

Sample	SiO <sub>2</sub>	TiO <sub>2</sub>	Al <sub>2</sub> O <sub>3</sub>	FeO <sub>t</sub>	MnO	MgO	CaO	Na <sub>2</sub> O	K <sub>2</sub> O	P <sub>2</sub> O <sub>5</sub>	Total	-Cl-
Roxolany #A1	71.25	0.05	12.87	0.65	0.04	0.05	0.95	3.36	4.36	0.04	93.62	0.21
#A2	71.45	0.10	13.19	0.68	0.05	0.07	1.04	3.40	4.23	0.05	94.26	0.19
#A3	72.05	0.07	13.23	0.72	0.02	0.10	1.08	3.83	4.25	0.01	95.36	0.16
#A4	71.09	0.09	13.01	0.62	0.08	0.05	0.86	3.79	4.82	0.02	94.43	0.20
#A5	73.34	0.10	13.08	0.64	0.00	0.06	0.98	3.80	4.38	0.06	96.44	0.17
#A6	73.53	0.06	12.99	0.51	0.00	0.02	0.87	3.76	4.78	0.02	96.54	0.17
#A7	71.01	0.06	12.86	0.58	0.05	0.04	0.98	3.75	4.16	0.04	93.53	0.17
#A8	72.37	0.09	12.96	0.66	0.03	0.04	0.94	3.28	4.42	0.03	94.82	0.19
#A9	73.40	0.07	12.72	0.61	0.02	0.05	0.90	3.28	4.62	0.00	95.67	0.21
#A10	74.02	0.08	13.07	0.56	0.01	0.01	0.87	3.99	4.32	0.00	96.93	0.16
#A11	72.50	0.09	12.92	0.69	0.03	0.05	1.03	3.45	4.50	0.08	95.34	0.17
#A12	73.39	0.06	12.04	0.61	0.03	0.06	0.87	2.96	4.53	0.00	94.55	0.13
#A13	72.60	0.09	12.90	0.54	0.05	0.04	0.92	3.47	4.39	0.00	95.00	0.22
#A14	72.22	0.06	12.83	0.50	0.03	0.04	0.92	3.34	4.26	0.00	94.20	0.15
#A15	72.92	0.10	12.81	0.74	0.05	0.06	0.93	3.44	4.49	0.04	95.58	0.20
<b>Mean</b>	<b>72.48</b>	<b>0.08</b>	<b>12.90</b>	<b>0.62</b>	<b>0.03</b>	<b>0.05</b>	<b>0.94</b>	<b>3.53</b>	<b>4.43</b>	<b>0.03</b>	<b>95.05</b>	<b>0.18</b>
<i>SD</i>	<i>0.93</i>	<i>0.02</i>	<i>0.27</i>	<i>0.07</i>	<i>0.02</i>	<i>0.02</i>	<i>0.07</i>	<i>0.27</i>	<i>0.19</i>	<i>0.02</i>	<i>1.87</i>	<i>0.02</i>
<i>Lipari Obsidian</i>												
15 µm-beam	74.07	0.08	13.18	1.67	0.05	0.05	0.72	4.09	5.15	0.00	98.96	0.31

**JEOL JXA-8230 (23/10/2014)**

Sample	SiO <sub>2</sub>	TiO <sub>2</sub>	Al <sub>2</sub> O <sub>3</sub>	FeO <sub>t</sub>	MnO	MgO	CaO	Na <sub>2</sub> O	K <sub>2</sub> O	P <sub>2</sub> O <sub>5</sub>	Total	-Cl-
Roxolany #B1	73.35	0.06	12.33	0.54	0.05	0.03	0.89	3.17	4.41	0.03	94.86	0.14
#B2	72.44	0.09	12.49	0.58	0.06	0.03	0.71	3.33	4.85	0.00	94.58	0.17
#B3	71.94	0.09	12.54	0.74	0.03	0.06	0.92	3.54	4.52	0.03	94.41	0.18
#B4	71.97	0.05	12.03	0.67	0.06	0.05	0.89	3.26	4.13	0.00	93.11	0.17
#B5	72.97	0.07	12.25	0.59	0.02	0.04	0.86	3.34	4.44	0.02	94.60	0.21
#B6	71.78	0.07	12.22	0.45	0.06	0.01	0.97	3.49	3.78	0.03	92.86	0.16
#B7	73.62	0.10	12.21	0.60	0.01	0.03	0.77	3.76	3.82	0.00	94.92	0.18
#B8	72.46	0.10	12.80	0.83	0.02	0.01	0.86	3.75	4.62	0.00	95.45	0.26
#B9	72.33	0.04	12.12	0.49	0.05	0.01	0.92	2.99	4.51	0.07	93.53	0.17
#B10	72.58	0.10	12.43	0.68	0.08	0.04	0.88	3.40	4.44	0.00	94.63	0.21
#B11	73.10	0.07	12.30	0.50	0.04	0.02	0.93	3.34	4.41	0.00	94.71	0.17
#B12	72.81	0.06	12.32	0.54	0.02	0.02	0.93	3.37	4.14	0.00	94.21	0.19
#B13	72.83	0.05	12.35	0.54	0.07	0.05	0.86	3.02	4.63	0.00	94.40	0.17
#B14	71.07	0.08	12.28	0.63	0.05	0.05	0.89	3.30	4.19	0.01	92.55	0.19
#B15	71.77	0.12	12.57	0.64	0.01	0.05	0.89	3.59	4.58	0.04	94.26	0.17
#B16	71.25	0.09	12.62	0.72	0.05	0.04	0.91	3.53	4.51	0.00	93.72	0.19
<b>Mean</b>	<b>72.39</b>	<b>0.08</b>	<b>12.37</b>	<b>0.61</b>	<b>0.04</b>	<b>0.03</b>	<b>0.88</b>	<b>3.39</b>	<b>4.37</b>	<b>0.01</b>	<b>94.18</b>	<b>0.18</b>
<i>SD</i>	<i>0.70</i>	<i>0.02</i>	<i>0.19</i>	<i>0.10</i>	<i>0.02</i>	<i>0.02</i>	<i>0.06</i>	<i>0.21</i>	<i>0.28</i>	<i>0.02</i>	<i>0.77</i>	<i>0.03</i>
<i>Lipari Obsidian</i>												
10 µm-beam	73.61	0.09	12.87	1.55	0.06	0.03	0.71	4.02	5.22	0.02	98.18	0.37
15 µm-beam	73.53	0.10	12.85	1.61	0.11	0.02	0.72	4.06	5.30	0.00	98.30	0.37
20 µm-beam	73.56	0.05	12.78	1.49	0.11	0.05	0.72	4.01	5.26	0.00	98.03	0.34

464

465

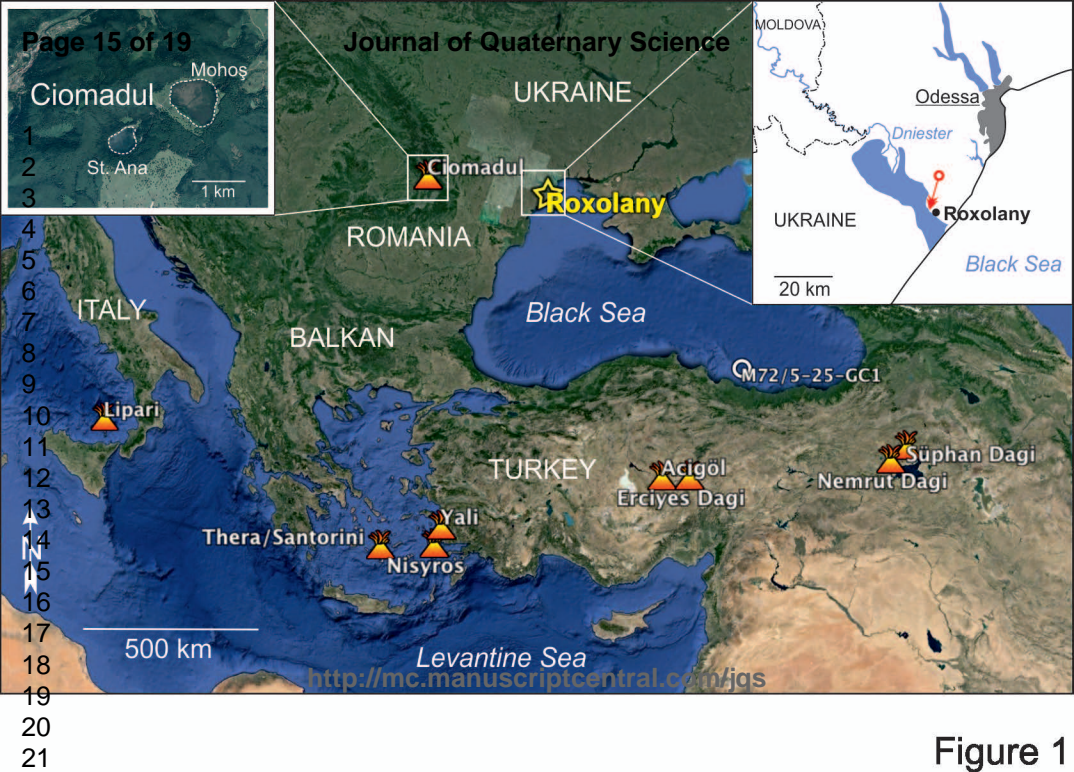
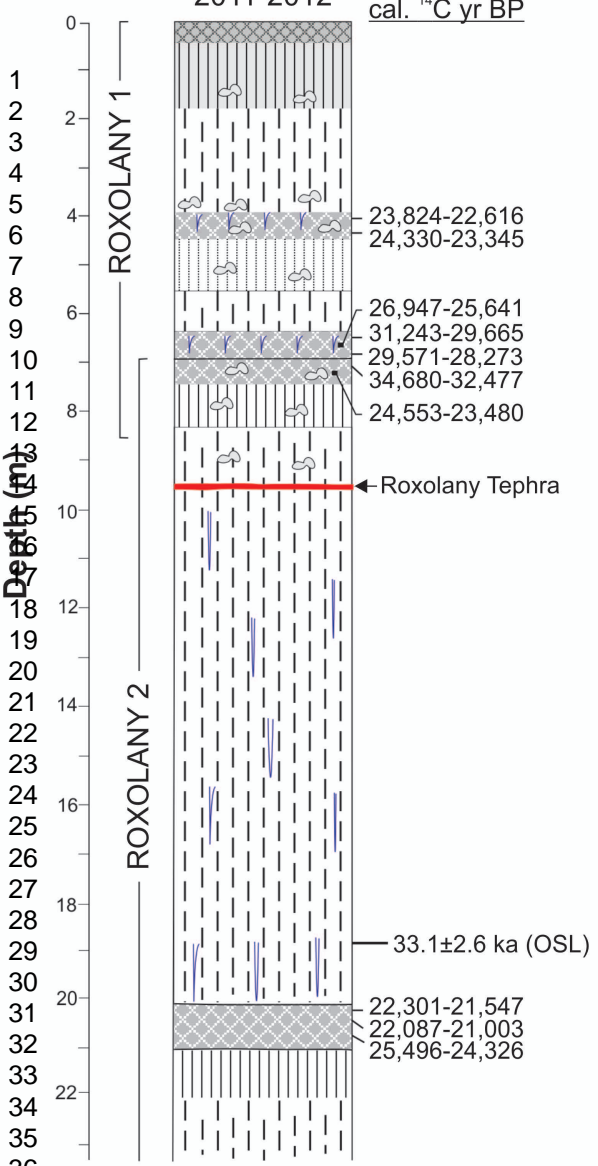


Figure 1



units	MIS
Modern soil	1
Fossil soil	Late glacial
Dofinivka set of soils (df)	2
Bug loess (bg)	
Vytachiv pedocomplex (vt)	3
Uday loess (ud)	4

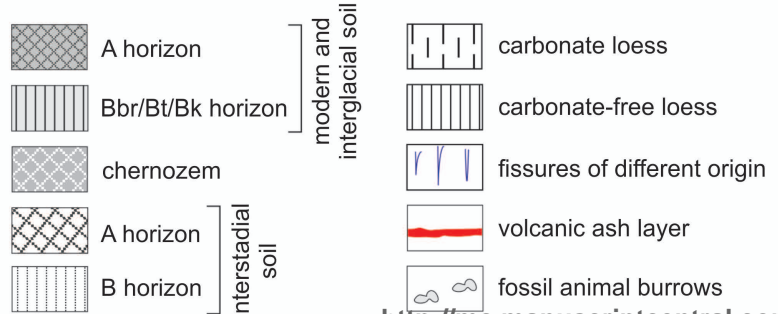
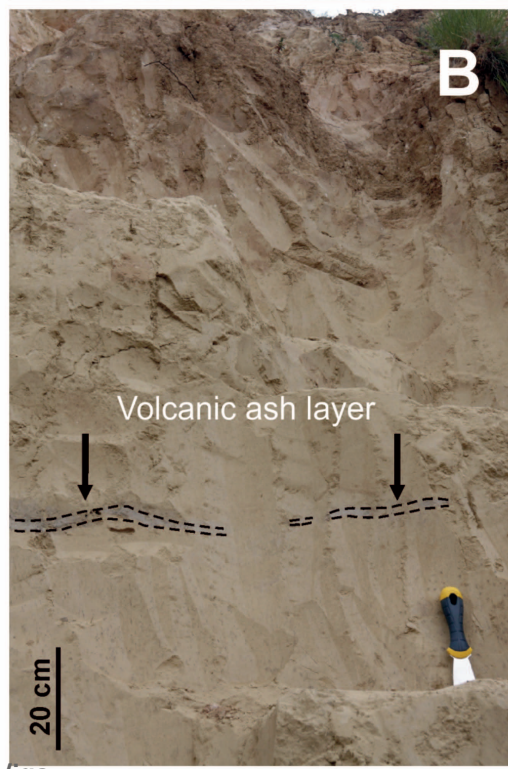
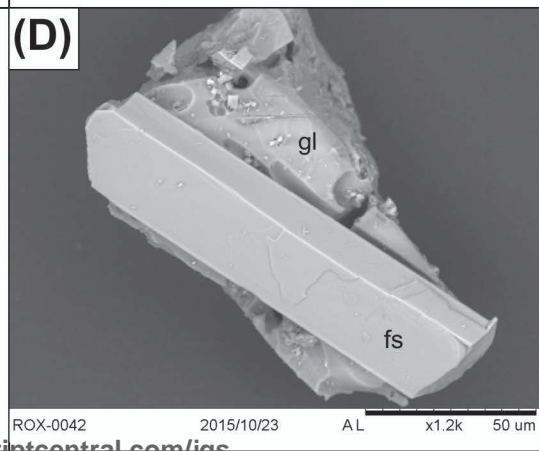
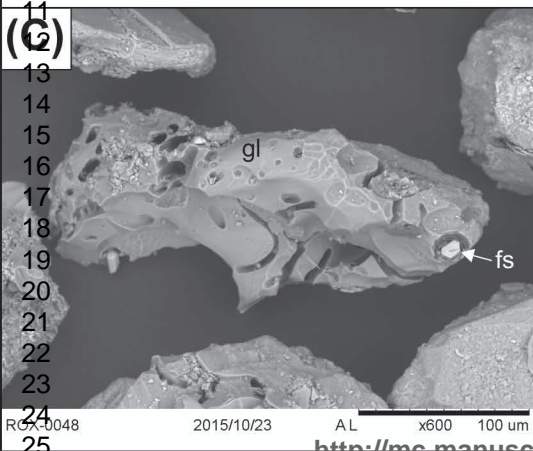
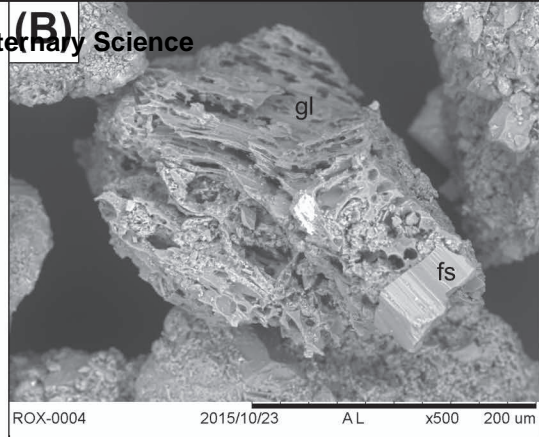
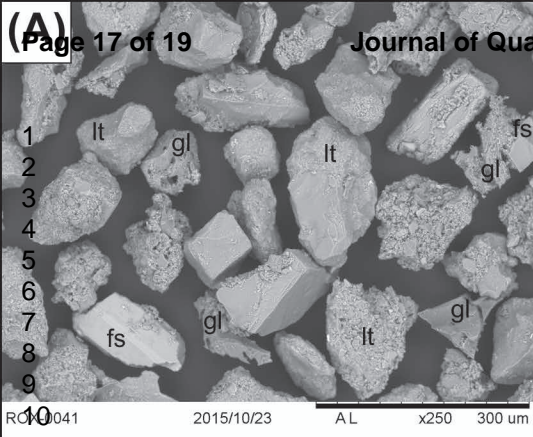
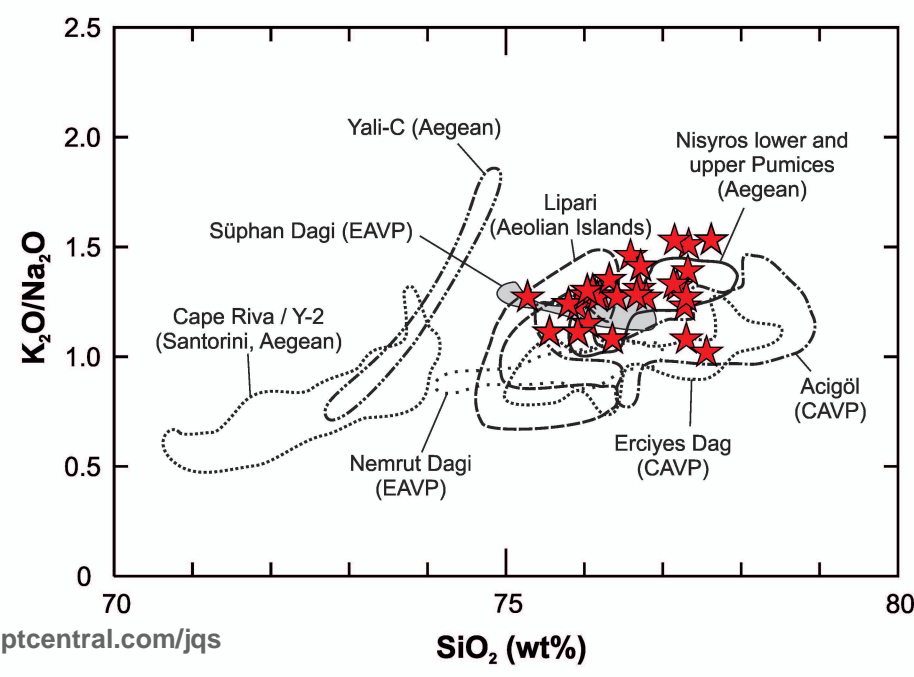
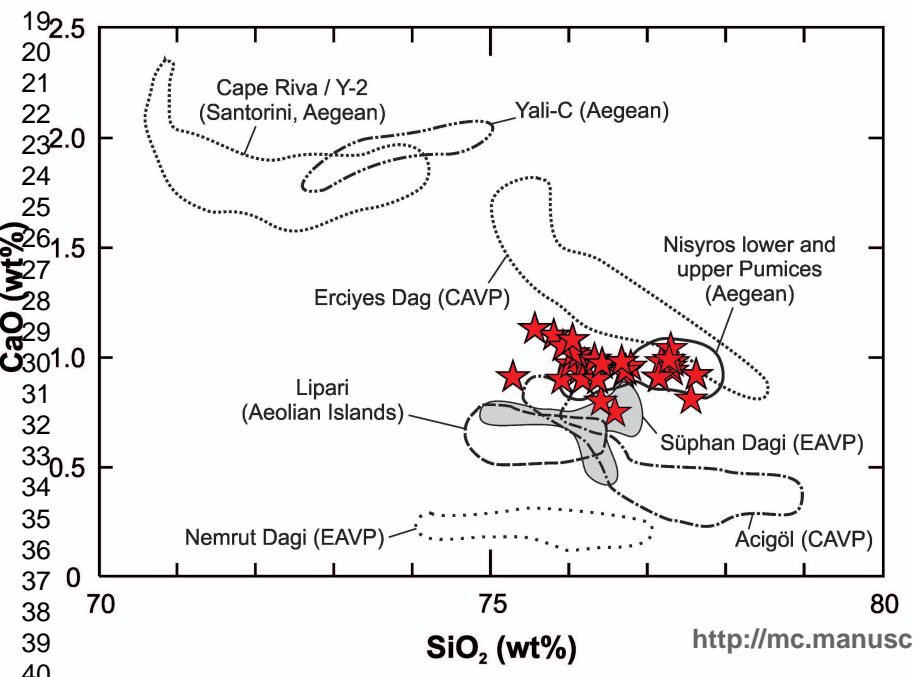
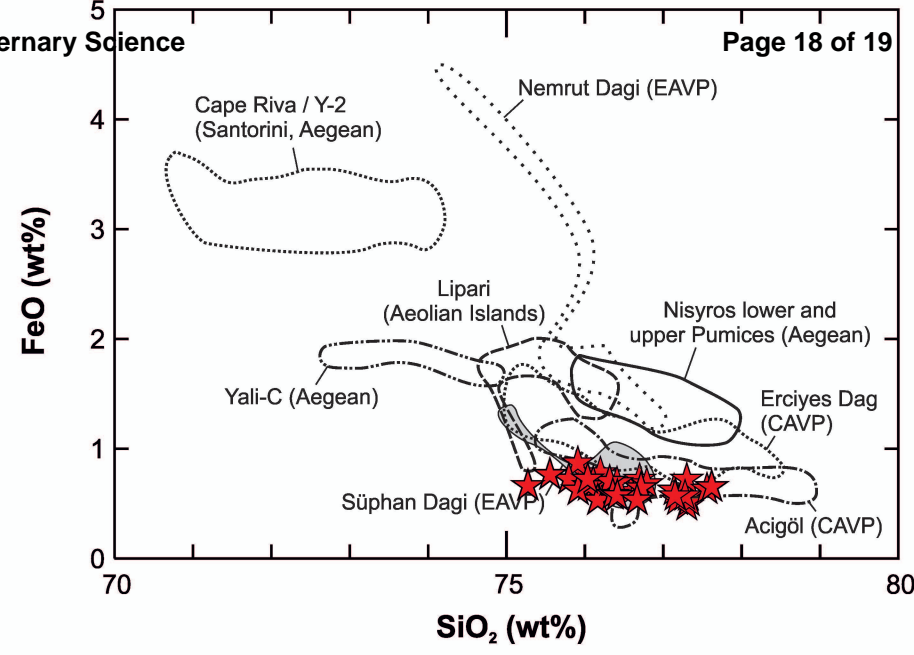
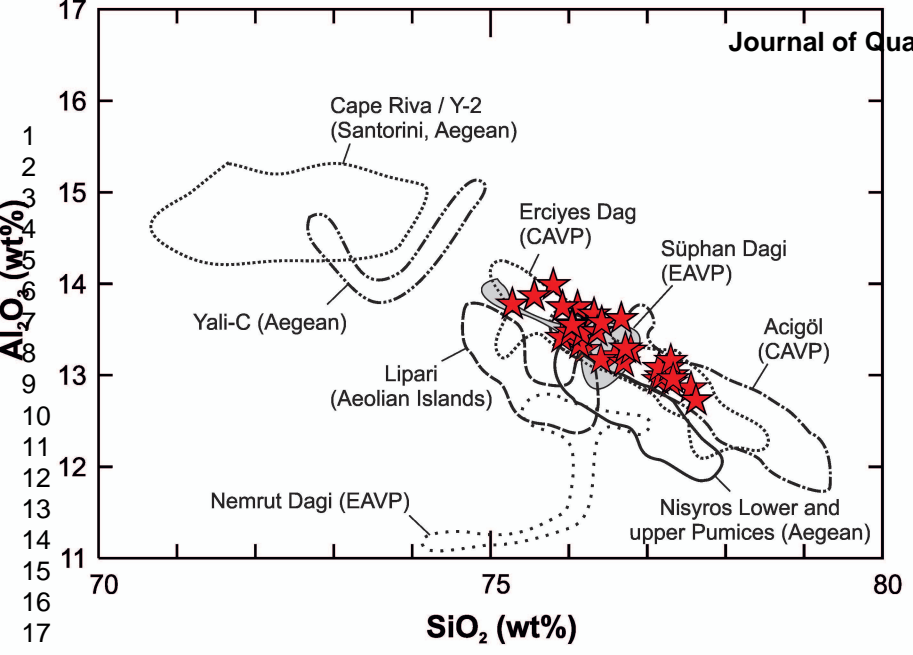


Figure 2



<http://mc.manuscriptcentral.com/jqs>

Figure 3



<http://mc.manuscriptcentral.com/jqs>

Figure 4

SiO<sub>2</sub> (wt%)

SiO<sub>2</sub> (wt%)

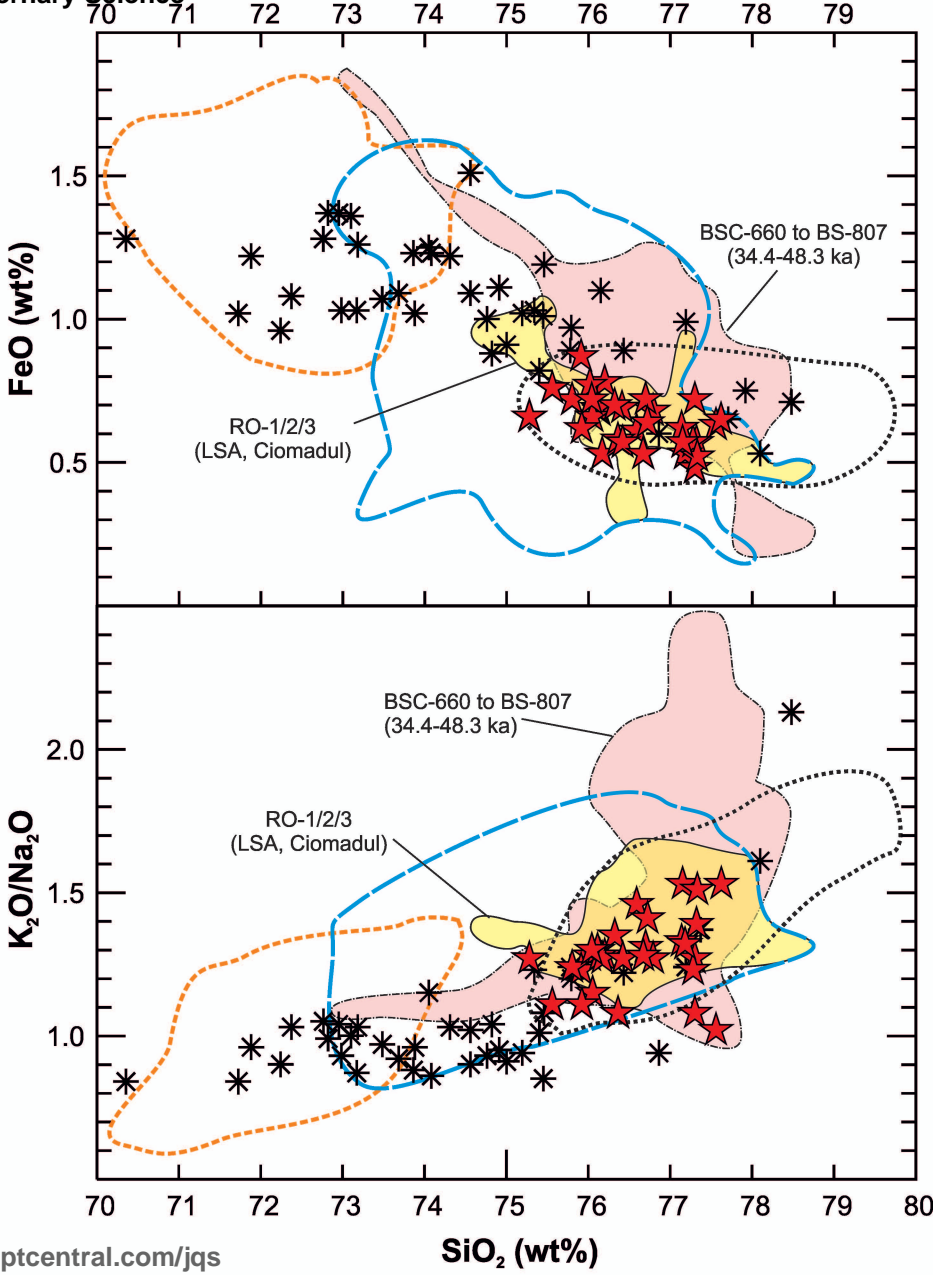
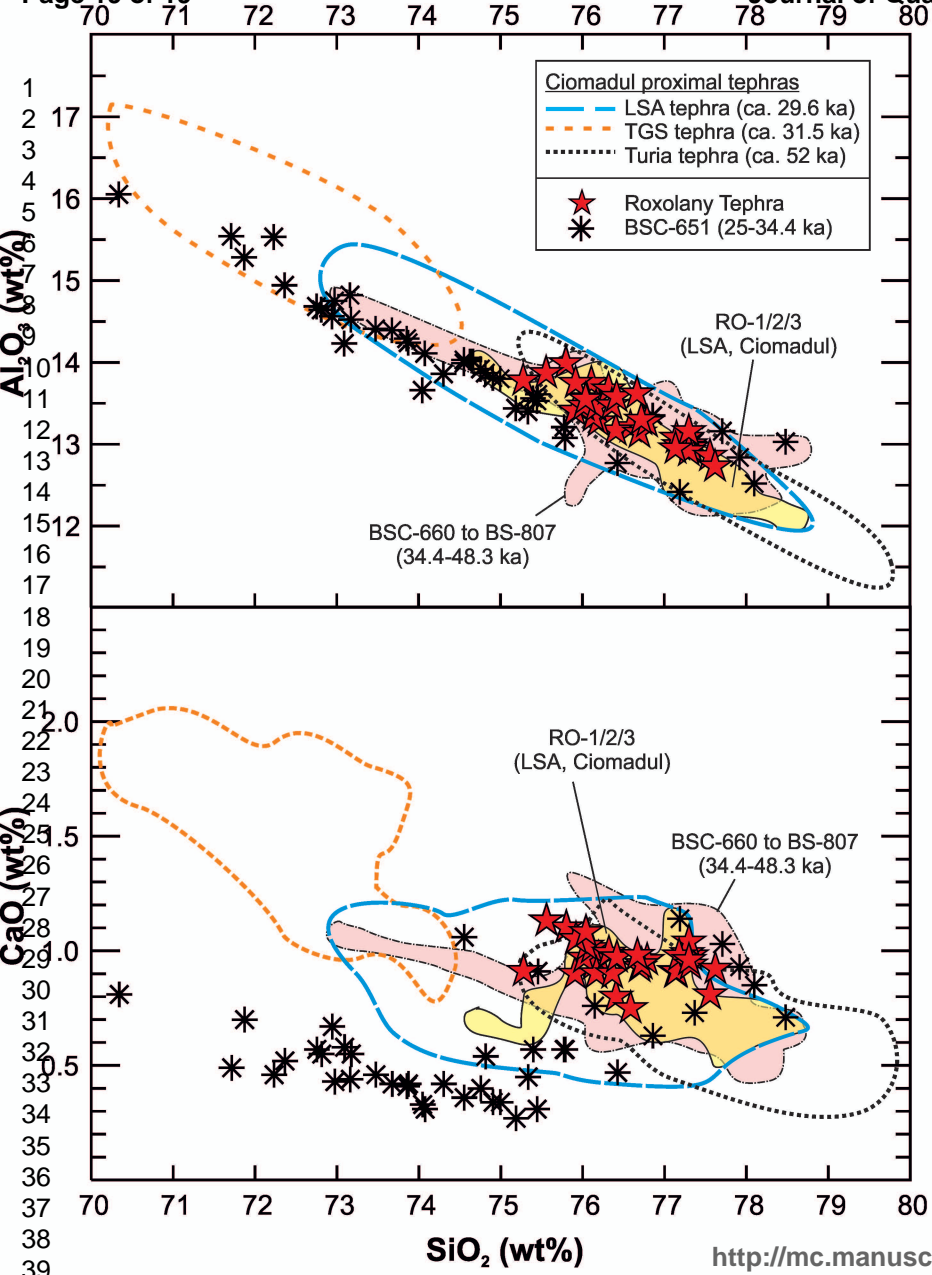


Figure 5